



شبكة المعلومات الجامعية

بِسْمِ اللَّهِ الرَّحْمَنِ الرَّحِيمِ



شبكة المعلومات الجامعية
@ ASUNET



شبكة المعلومات الجامعية التوثيق الالكتروني والميكرو فيلم



شبكة المعلومات الجامعية

جامعة عين شمس

التوثيق الالكتروني والميكروفيلم

قسم

نقسم بالله العظيم أن المادة التي تم توثيقها وتسجيلها
علي هذه الأفلام قد أعدت دون أية تغيرات



يجب أن

تحفظ هذه الأفلام بعيدا عن الغبار

في درجة حرارة من ١٥-٢٥ مئوية ورطوبة نسبية من ٢٠-٤٠%

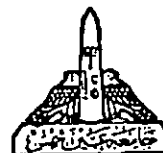
To be Kept away from Dust in Dry Cool place of
15-25- c and relative humidity 20-40%

بعض الوثائق الأصلية تالفة

بالرسالة صفحات لم ترد بالاصل

BVE91

Ain Shams University
Faculty of Girls
For
Arts, Science and Education



STRUCTURE AND PHYSICAL PROPERTIES OF CADMIUM GALOSELENIDE FILMS AND THE OPTIMUM CONDITIONS FOR SUITABLE ELECTRONIC APPLICATIONS

A Thesis

**Submitted For The Ph.D. Degree of Philosophy
In Science (Physics)**

By

Eman Hashem Aly Hassan

Master in Science

Supervised BY

Prof. Dr. M.M.H. EI-NABY
Physics Department
Faculty for Girls
Ain Shams University

Prof. Dr. T.A. HINDIA
National Research Center

Dr. H.S. SOLIMAN
Ass. Prof. Physics Department
Faculty of Education
Ain Shams University

Dr. H.M. ABO DORRA
Ass. Prof. Physics Department
Faculty for Girls
Ain Shams University

July 1995

Ain Shams University
Faculty of Girls for
Arts, Science and Education

Name of Student : EMAN HASHEM ALY HASSAN

Master In Science

Title of Thesis : Structure and Physical Properties of Cadmium
Galoselenide Films and The Optimum Conditions
for Suitable Electronic Applications.

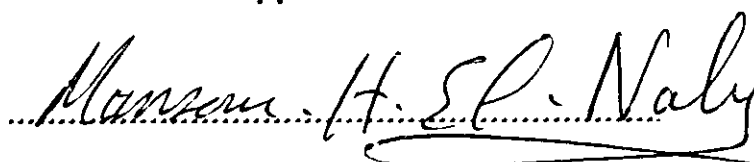
Supervised by :

Approved

Prof. Dr. M.M.H. EI-NABY

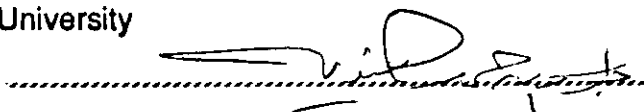
Physics Department

Faculty of Girls - Ain Shams University



Prof. Dr.T.A. HINDIA

National Research Center

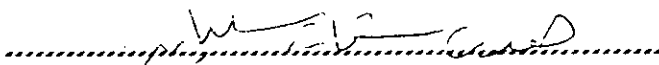


Dr. H.S. SOLIMAN

Ass. Prof. Physics Department

Faculty of Education

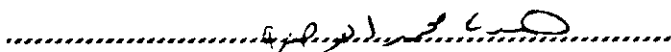
Ain Shams University



Dr. H.M ABO DORRA

Ass. Prof. Physics Department

Faculty of Girls - Ain Shams University



CONTENTS

PAGE

LIST OF FIGURES

LIST OF TABLES

ACKNOWLEDGEMENT

ABSTRACT

SUMMARY

CHAPTER I : INTRODUCTION AND LITERATURE REVIEW

1.1) Introduction	1
1.2) Growth of CdGa ₂ Se ₄ Crystals	3
1.3) Structural Characterization of CdGa ₂ Se ₄	4
1.4) Aspects of The Band Structure of CdGa ₂ Se ₄	5
1.5) Optical Properties of CdGa ₂ Se ₄	9
1.6) Transport Properties of CdGa ₂ Se ₄	16

CHAPTER II : THEORETICAL BACKGROUND

2.1) Structure Features of $\overset{\text{II}}{\text{A}} \overset{\text{III}}{\text{B}_2} \overset{\text{IV}}{\text{B}_4}$ Compounds	22
2.1.1- Structure Features of CdGa ₂ Se ₄	26
2.2) Theoretical Determination of the optical constants of thin films	26
a- Bennett and Booty method	28
b- Abelés and Théye's method	29
c- Algebraic inversion methods.	30
d- Envelope methods	30
2.3) Activation Energies For Electronic Conduction	31
2.3.1- Intrinsic Semiconductor	31

2.3.2- Extrinsic Semiconductor	32
I- Uncompensated Case	32
II- Compensated Case	33
2.3.3- Pseudo-Intrinsic or non-extrinsic conduction	35
2.3.4- Meyer-Neldel rule	37
2.4) Thermoelectric Power	39
2.5) Heterojunctions	40
 CHAPTER III : EXPERIMENTAL TECHNIQUES	
3.1) Preparation of CdGa₂Se₄ in Bulk form	44
3.2) Preparation of Thin Films of CdGa₂Se₄	45
3.2.1- Cleaning of the substrate surface.	48
3.2.2- Deposition technique	48
3.3) Film Thickness Measurement	50
3.1.1- Quartz crystal thickness monitor	50
3.3.2- Multiple beam interferometry	51
3.3.3- Envelope method	53
3.4) Structure Characterization Techniques	55
3.4.1- X-ray diffraction	55
3.4.2- Electron microscopy technique	56
3.4.2.1- Preparation of CdGa ₂ Se ₄ thin films for electron microscope examination	56
3.5) Determination of The Optical Constants of Absorbing Films on Transparent Substrates	57
3.5.1- The transmittance at normal light incidence	58
3.5.2- The reflectance at normal light incidence	58
3.5.3- Computing the optical constants of thin films.	59

3.6) Electrical Resistivity Measurements	64
3.7) Thermoelectric Power Measurements	65
3.8) CdGa₂Se₄ /Si Heterojunctions	69
3.8.1- Preparation of CdGa ₂ Se ₄ /Si heterojunctions	69
3.8.2- Current-voltage measurements of heterojunctions	69

CHAPTER IV : STRUCTURE CHARACTERIZATION OF CdGa₂Se₄

4.1) Structure Investigation of CdGa₂Se₄ Ingot Material	71
4.2) Structure Characterization of As-deposited CdGa₂Se₄ Thin Films	77
4.3) Effect of Heat Treatment on the Structure Charac- terization of CdGa₂Se₄ Thin Films	82
4.4) Effect of Heat Treatment on the Crystallite Size of CdGa₂Se₄ Thin Films	87

CHAPTER V : OPTICAL PROPERTIES OF CdGa₂Se₄ THIN FILMS

5.1) The Spectral Distribution of Transmittance and Reflectance	99
5.2) The Spectral Distribution of Absorption Coefficient	103
5.3) The Spectral Distribution of the Refractive Index and the Dielectric Constant.	109

CHAPTER VI : TRANSPORT PROPERTIES OF CdGa₂Se₄ THIN FILMS

6.1) The Electrical Conductivity of CdGa₂Se₄ Thin Films	116
--	------------

6.1.1- Current-voltage characteristics of CdGa ₂ Se ₄ thin films	116
6.1.2- The volume and surface conductivities of CdGa ₂ Se ₄ thin films	120
6.1.3- The electrical conductivity of CdGa ₂ Se ₄ in bulk form	123
6.1.4- The effect of thickness on the surface electrical conductivity of CdGa ₂ Se ₄ thin films	126
6.1.5- The effect of annealing on surface electrical conductivity of CdGa ₂ Se ₄ thin films	131
6.2) The Thermoelectric Power of CdGa₂Se₄ Thin Films	137
6.3) The Electrical Characteristics of p-CdGa₂Se₄/n-Si Heterojunctions	145
GENERAL CONCLUSIONS	162
REFERENCES	168
ARABIC SUMMARY	

LIST OF FIGURES

- Fig. (1.1) : The model of the valence band of CdGa_2Se_4 at the Γ point of the Brillouin zone (Δ_{SO} : spin-orbit interaction).
- Fig. (1.2) : Transmission spectra of CdGa_2Se_4 grown from different starting materials (a) and two binary compounds of CdSe and Ga_2Se_3 with stoichiometric or nonstoichiometric compositions (b).
- Fig. (1.3) : Temperature dependence of electrical conductivity and thermoelectric power for CdGa_2Se_4 single crystal.
- Fig. (2.1) : Chalcopyrite family and related compounds in which the individual atomic species may be replaced by others of similar valence.
- Fig. (2.2) : Defect chalcopyrite structure of CdGa_2Se_4 .
- Fig. (2.3) : Schematic energy level diagram for a solid in which the dominant electron and hole states are labelled (m) and (q) respectively.
- Fig. (2.4) : (a) Energy-band diagram for two isolated n- and p-type semiconductors.
(b) Energy -band diagram of p-n heterojunction at equilibrium according to Anderson model.
- Fig. (3.1) : Rotating furnace.
- Fig. (3.2) : Schematic diagram of coating system.
- Fig. (3.3) : Typical interferometer arrangement.
- Fig. (3.4) : Schematic diagram of multiple-beam interferometry.
- Fig. (3.5) : Fringes produced by multiple-beam interferometry across a film substrate step.
- Fig. (3.6) : Simplified optical path of the V-W specular reflection;
Schematic (A) in the V case and (B) in the w case.
- Fig. (3.7) : Flow chart diagram of the program used for the optical constants calculations.

- Fig. (3.8) : Plot of the variance versus refractive index, n for different values of absorption index, k [T_{exp} , R_{exp} and t/λ are kept constant].
- Fig. (3.9) : Schematic diagram of the electrical circuit for measuring the film resistance.
- Fig. (3.10) : Schematic diagram of the circuit used for measuring the electromotive force.
- Fig. (3.11) : Sketch of $\text{CdGa}_2\text{Se}_4/\text{Si}$ heterojunction.
- Fig. (3.12) : The electrical circuit used for measuring the current-voltage characteristics of heterojunction.
- Fig. (4.1) : The atomic scattering factor, for (a) Ga, (b) Se and c) Cd element plotted against $\sin \theta/\lambda$.
- Fig. (4.2) : (a) The Debye-Scherrer pattern for CdGa_2Se_4 in powder form.
(b) The calculated relative intensities of X-ray diffraction pattern of CdGa_2Se_4 in powder form ($\text{CuK}\alpha$ line was used).
- Fig. (4.3) : XRD pattern of as-deposited CdGa_2Se_4 film of thickness 580 nm.
- Fig. (4.4-6) : Electron microscope diffraction patterns of as-deposited CdGa_2Se_4 thin films of thicknesses 30, 40 and 50 nm respectively.
- Fig. (4.7-9) : TEM micrograph as-deposited CdGa_2Se_4 thin films of thicknesses 30, 40 and 50 nm respectively [magnification = 25000 X].
- Fig. (4.10) : XRD patterns of CdGa_2Se_4 films of 580 nm thick : (a) as-deposited film; and films annealed at (b) 473 K, (c) 573 K, (d) 623 K, and (e) 673 K, (f) XRD pattern of CdGa_2Se_4 in powder form.
- Fig. (4.11) : (a-c) XRD patterns of CdGa_2Se_4 films of nearly equal thicknesses ≈ 270 nm deposited at substrate temperatures of (a) 300 K, (b) 523 K and (c) 573 K, (d) XRD pattern of CdGa_2Se_4 in powder form.
- Fig. (4.12,13) : Electron microscope diffraction patterns of CdGa_2Se_4 film of thickness 35 nm deposited at $T_s = 300$ K and 573 K respectively.

- Fig. (4.14) : X-ray line broadening of the (112) reflection for CdGa_2Se_4 in powder form.
- Fig. (4.15) : X-ray line broadening of the (112) reflection for CdGa_2Se_4 thin film of thickness 580 nm annealed at $T_A = 598$ K.
- Fig. (4.16) : X-ray line broadening of the (112) reflection for CdGa_2Se_4 thin film of thickness 580 nm annealed at $T_A = 623$ K.
- Fig. (4.17) : X-ray line broadening of the (112) reflection for CdGa_2Se_4 thin film of thickness 580 nm annealed at $T_A = 673$ K.
- Fig. (4.18) : X-ray line broadening of the (112) reflection for CdGa_2Se_4 thin film of thickness 270 nm prepared at $T_S = 573$ K.
- Fig. (4.19,20) : TEM micrographs of CdGa_2Se_4 thin film of thickness 35 nm deposited at $T_S = 300$ and 573 K respectively [magnification = 25000 X].
- Fig. (5.1) : The spectral behaviour of the transmittance $T(\lambda)$ and reflectance $R(\lambda)$ at normal incidence for as-deposited CdGa_2Se_4 films of different thicknesses.
- Fig. (5.2) : The spectral behaviour of the transmittance $T(\lambda)$ and reflectance $R(\lambda)$ at normal incidence for CdGa_2Se_4 films of different thicknesses deposited onto preheated substrates $T_S = 573$ K.
- Fig. (5.3) : The spectral behaviour of the transmittance $T(\lambda)$ and reflectance $R(\lambda)$ at normal incidence for CdGa_2Se_4 films of different thicknesses and annealed at $T_A = 623$ K for two hours.
- Fig. (5.4) : The spectral distribution of absorption index, $k(\lambda)$ of CdGa_2Se_4 films
(A) as-deposited.
(B) [o] $T_A = 623$ K (open circle) and [•] $T_S = 573$ K (solid circle).

- Fig. (5.5) : The spectral behaviour of the absorption coefficient, α
(A) as-deposited.
(B) Same as in Fig. 5.4(B).
- Fig. (5.6) : $(\alpha h\nu)^{1/2}$ plotted against $(h\nu)$:
(A) as-deposited
(B) Same as in Fig. 5.4(B).
- Fig. (5.7) : $(\alpha h\nu)^2$ plotted against $(h\nu)$:
(A) as-deposited
(B) Same as in Fig. 5.4(B).
- Fig. (5.8) : $\log(\alpha h\nu)$ plotted against $\log(h\nu - E_g)$ for as-deposited CdGa_2Se_4 thin films
- Fig. (5.9) : The spectral distribution $n(\lambda)$ of CdGa_2Se_4 films :
(A) as-deposited
(B) Same as in Fig. 5.4(B).
- Fig. (5.10) : $(n^2 - 1)^{-1}$ plotted against λ^{-2} in wavelength range 540-840 nm :
(A) as-deposited
(B) Same as in Fig. 5.4(B).
- Fig. (6.1) : $\log I$ vs. $\log V$ for a sample C_1 of thickness 326.8 nm deposited at $T_s = 573$ K. The measurement was performed for $\text{Au}/\text{CdGa}_2\text{Se}_4/\text{Au}$ configuration at room temperature.
- Fig. (6.2) : $\log I$ vs $V^{1/2}$ in high field region for the sample C_1 .
- Fig. (6.3a) : The temperature dependence of the conductivity for the sample C_1 in sandwich configuration.
- Fig. (6.3b) : The temperature dependence of the conductivity for the sample C_1 in coplanar configuration.
- Fig. (6.4) : The temperature dependence of the conductivity for CdGa_2Se_4 in bulk form.